BALKANTRIB'O5
5th INTERNATIONAL CONFERENCE ON TRIBOLOGY
JUNE.15-18. 2005
Kragujevac, Serbia and Montenegro

NEW EXPERIMENTAL DATA MEASURED ON A TWO DISK RIG

Petre Lucian SEICIU, Dan PAVELESCU

Department of Machine Elements and Tribology, "Politehnica" University Bucharest, Romania.

Keywords: elastohydrodynamic lubrication, hertzian line contact

1. INTRODUCTION

The elastohydrodynamic (EHD) lubrication, as the mainframe of the present paper, was studied by several authors (only partially quoted further on) and specially in these main aspects:

the theory of the EHD regime [1-3]; the rheological effect of the viscosity variation with temperature and pressure in the contact zone [3-8];

the theory of liquid-solid lubrication in EHD regime [1-6];

the EHD film thickness [1, 4, 6-11];

traction in EHD regime [17-22];

the measurement technique of the lubricant film response to pressure, velocity, temperature in the EHD regime [1, 4, 6-13].

Several authors agreed that, while passing through the contact zone, the film thickness and rheology of the lubricant depend specially on pressure and temperature. The passing time through contact is very short (10^{-4} – 10^{-6}s) with a state change of the lubricant (from liquid to solid and back to liquid) [1-6].

The two main parameters of the EHL regime (film thickness and traction) depend on several factors: oil properties, surface roughness, materials, speed, load etc [6-9]. Until now, all these influences were studied only while loading. This paper presents some interesting results observed during a complete cycle of loading and unloading, similar to the real functioning.

2.THE EXPERIMENTAL INSTALATION

Several papers presented various possibilities and testing rigs for the measurement of the film thickness and of the corresponding EHD regime. It is interesting to remark that for measuring the oil viscosity variation with the pressure, initially were used rollers functioning at pressures of 0.8-1.2 GPa [2, 6-9], than plane contacts and, lately, line contacts (two or four disk rigs) [2, 5-8].

The experimental results used in this paper were measured on a complex two-disk installation with an electrical resistance device for film thickness measurement, presented in [8]. The rig allows the variation of several parameters: load, rolling speed, rolling and sliding speed, temperature. The parameters measured are the film percent and the friction coefficient and the results can be observed directly on an oscilloscope, read on a digital multimeter, recorded on paper by an oscillograph or stored electronically by a data acquisition device. Also, the results can be presented as instant values or as mean values on a desired period, using a time integrator device.

All the experiments presented in this paper were made using:

- an extreme pressure additivated mineral oil for gears with the dynamic viscosity $\eta_0 = 0.441$ Pa·s at 20 °C, the temperature coefficient $\beta = 0.076$ °C^{-1} and the pressure coefficient $\alpha = 2.15$ GPa^{-1};
- the disks were made of hardened steel and had the roughness $R_a = 1.156$ μm and $R_z = 1.071$ μm.

We stress that the measurements were made very carefully in order to obtain an error margin less than 2%.

3. NEW EXPERIMENTAL RESULTS

3.1. The measurements were made by increasing the load (loading) step by step, up to a maximum value (corresponding to $P_{H,max} = 1.2$ GPa), followed by the decreasing of the load (unloading), at the same steps, down to zero and, also, for various values of speed (between 9 m/s to 35 m/s) and temperature (ranging from 40 to 90 ^{O}C).

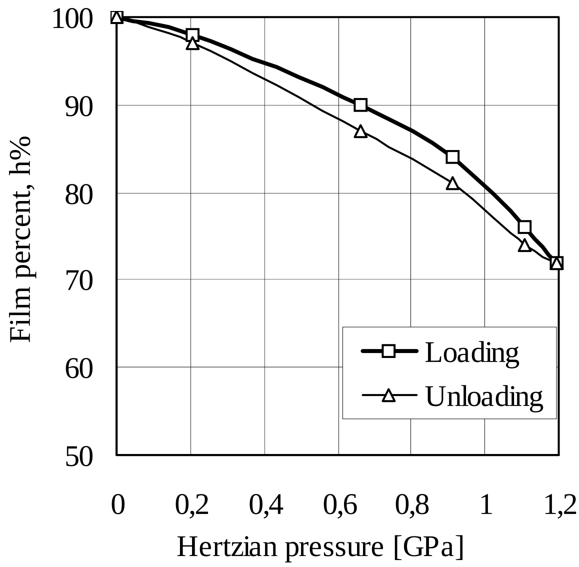

Figure 1: *Load influence on film percent*

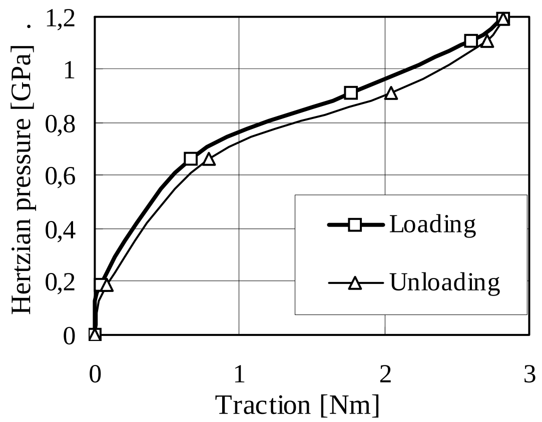

Figure 2: *Load influence on traction*

3.2 The film thickness measured on the installation presents a rheological phenomenon of hysteresis loop during the process of uploadig followed by downloading. We name this phenomenon *"rheological hysteresis"* (RH) and it is presented in Figure 1 as a SKF type diagram.

3.3 The traction measured on the installation presents also a rheologic phenomenon of hysteresis loop during the process of uploadig followed by downloading. The diagrams presented in the figures 1 and 2 are plotted for the rolling speed v_r = 11.2 m/s and the temperature of 40 ^{O}C.

3.4. For the film thickness, we propose to change the presentation from this classical SKF form (in Figure 1) to the one in Figure 3.

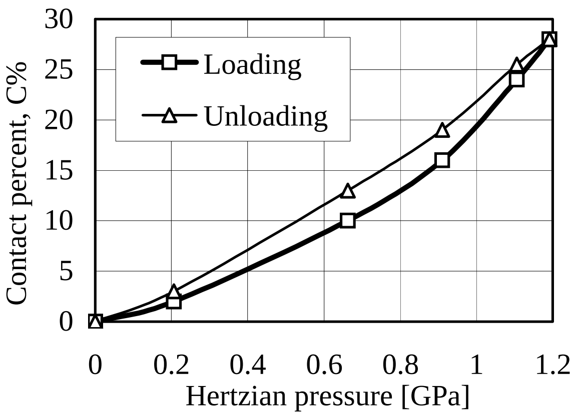

Figure 3: *Load influence on film contact*

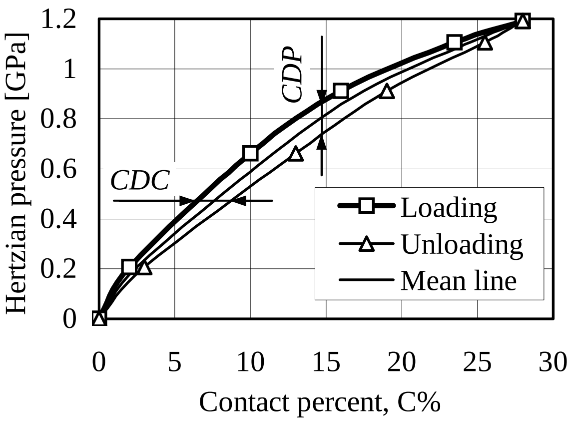

Figure 4: *Load influence on film contact (reversed axes)*

This change allows a better presentation of the observed RH phenomenon by replacing film percent (h%) with the term contact percent, C%, defined as:

$$C\% = \left(1 - \frac{h\%}{100}\right) \cdot 100 \qquad (1)$$

Figure 4 shows a better presentation of the RH aspect by reversing the axes.

3.5. The authors present a new parameter: absolute rheological contact deflection, CD and, respectively, relative rheological contact deflection, Δ_{CD}. This new parameter is used for measuring the variations of the contact hysteresis.

The contact deflection can be measured in two directions:

on the pressure axis results the absolute and the relative contact deflection related to pressure CDP and Δ_{CDP};

along the contact axis results the absolute and the relative contact deflection related to contact percent CDC and Δ_{CDC}.

This deflections are defined as:

$$\Delta_{CDP} = \frac{CDP}{P_{H,max}} \qquad (2)$$

$$\Delta_{CDC} = \frac{CDC}{C\%_{max}} \qquad (3)$$

where $P_{H,max}$ is the maximum Hertzian pressure, in this case $P_{H,max}$ = 1.2 GPa (Figure 4) and C_{max} is the maximum contact percent (corresponding to the maximum pressure $P_{H,max}$) for the hysteresis loop.

The total absolute and relative rheological contact deflection, CD and Δ_{CD}, are computed on the mean line, measuring the absolute deflections on both axes in the same point with:

$$CD = \sqrt{CDP^2 + CDC^2} \quad \text{and} \qquad (4)$$

$$\Delta_{CD} = \sqrt{\left(\frac{CDP}{P_{H,max}}\right)^2 + \left(\frac{CDC}{C\%_{max}}\right)^2} \qquad (5)$$

where $C\%_{max}$ is the maximum traction corresponding to the maximum Hertzian pressure $P_{H,\,max}$.

3.6. For the contact percent we present another new parameter: aria of the contact hysteresis loop, A_{CL}, respective, relative aria of the contact hysteresis loop, Δ_{ACL}.

$$A_{CL} = \int_0^{P_{H,\,max}} f_{CL}(p)dp - \int_0^{P_{H,\,max}} f_{CU}(p)dp \qquad (10)$$

$$\Delta_{ACL} = \frac{A_{CL}}{\int_0^{P_{H,\,max}} f_{Cm}(p)dp} \cdot 100\,\% \qquad (11)$$

where f_{CL} and f_{CU} are the functions that estimate the contact percent variation with pressure at loading and, respectively, at unloading and f_{Cm} is the function that estimates the mean contact variation with pressure.

3.7. Figure 5 shows the contact percent variation with Hertzian pressure and is plotted for the rolling speeds of 31 m/s and three different temperatures.

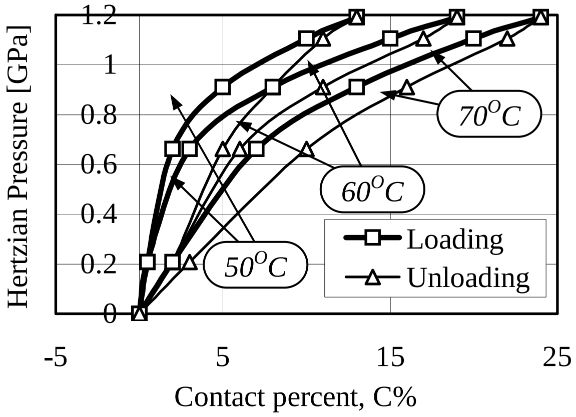

Figure 5

The RH phenomenon can be clearly observed and it depends on temperature and rolling speed.

The measurements were made by increasing the load (upload) step by step, up to a maximum value (corresponding to $P_{H,max} = P_1 = 1.2$ GPa), followed by the decreasing of the load (download), at the same steps, down to zero. Also, the experiments were made for various values of speed (between 9 m/s to 35 m/s) and temperature (ranging from 40 to 90 ^{O}C).

Observations:

• The rolling speed has a non-linear influence on RH: at medium speeds RH is larger than at low or high rolling speeds.

• The contact percent decreases with the speed increase as seen in the Figures 3, 4 and 5 where are plotted the curves for the same temperature (50°C), but for various speeds.

• The temperature has a direct influence on HR, but also influences the contact percent and, through it, the temperature seems to have also an indirect influence on HR.

• The temperature increase leads to a contact percent increasing (film percent decreasing) as shown in Figures 6 and 7 which are plotted for the same rolling speed $v_r = 26.8$ m/s and $v_r = 31$ m/s, respectively, but for three different temperatures (50°C, 60°C and 70°C).

4. PHENOMENON EXPLANATION

4.1. One explanation for the observed phenomenon will take into account the sonicity theory. The S.A.E. installation with EHD fluid film can be compared with an energy pulsating system with membrane, imagined originally by the Romanian scientist George Constantinescu.

He was the first to demonstrate and to use water and oil compressibility [11], presented in his sonicity theory.

In our case, the rheological hysteresis effect can be explained by the accumulation of the energy in the fluid film, periodically, but in a very short time (about $10^{-5} – 10^{-6}$ s).

The energy dispersion appears at the pressure reduction (during download), with a certain delay due to the rheological inertia.

4.2. Another explanation of this behavior must take into account the thermal problem in the contact. For a proper evaluation (both qualitative and quantitative) of this rheological phenomenon it must be considered the way the heat is generated in the contact, at loading, and its dissipation speed while unloading.

Conclusions

A complex SAE equipment was used for the line film thickness study and, for the first time, several phenomena were observed.

• The film thickness and traction behavior was studied on a complete loading-unloading cycle.

• A hysteresis type phenomenon, we called rheological hysteresis, appears only in the full EHD lubricant film. This phenomenon is similar with the hysteresis loop of elastic materials with inner friction or with the one of some electric circuits.

• For an easier study of this phenomenon, a new representation was proposed: contact percent–load diagram.

• Also there were defined the rheological hysteresis parameters: *hysteresis loop area* and *rheologic deflection*. Their behavior was studied related to various parameters: load, speed and temperature.

We consider this an interesting approach and also an easy way to study the rheological behavior of the fluids and we suggest to other researchers to follow it.

The authors would be grateful for any suggestions and shared experience.

5. REFERENCES

[1] B.O. JAKOBSON, Rheology and Elastohydrodynamic Lubrication, Elsevier, Amsterdam-Oxford-New York-Tokyo, 1991.

[2] S. BaIR, W.O. Winer Some Observations in High Pressure Rheology of Lubricants, J. Lub. Tech. **104**, p.357-364, 1982.

[3] S. BaIR, m. khonsari, W.O. Winer High-pressure Rheology of Lubricants and Limitations of the Reynolds Equation, Tribology International **31**, No. 10, p.573-586, 1998.

[4] V.N. CONSTANTINESCU, On the Viscosity of Fluids at High Pressures, Proc. of the VAREHD-1, Suceava, 1980.

[5] E.N. DIACONESCU, A Simple Model of Liquid Viscosity, EUROTRIB'89, Helsinki, p.136-141, 1989.

[6] R. ZECHEL, J.W. BARTZ, Pressure Viscosity of a Multigrade Engine Oils and Different Synthetic Lubricants, EUROTRIB'89, Helsinki, p.111-125, 1989.

[7] D. PAVELESCU, Some Theoretical and Experimental Researches on the Lubricant's Rheology within an EHD Contact, VAREHD'92, Suceava, p.13-24, 1992.

[8] P.L. SEICIU, Contributions at the Improvement of the Elastohydrodynamic Capacity of the Gears Modeled by Disks, PhD. Thesis, Bucharest, "POLITEHNICA" University Bucharest, 1997.

[9] e. kuss, Zur Frage des Viscositäts-DruckVerhaltensvon Öil, Erdoel Zeitschrifts, **78**, p. 628-688, Dez. 1962.

[10] a.t.j mayward, Measuring the Compressibility of Liquids, ACTA IMECO, Stockholm, p.249-272, 1964.

[11] g. CONSTANTINESCo, Sonics, The Transactions, Soc. of Engineers, p. 69-102, June 1959.

[12] A. N. GRUBIN Fundamentals Of The Hydrodynamic Theory Of Lubrication Of Heavily Loaded Cylindrical Surfaces, Moscow, Tsentral Nauk, Issledovatel, Inst. Teknol Mashinosteonen, 1949.

[13] P. L. SEICIU, New Aspects Of The EHD Lubrication Of The Line, T. C. M. M. 18, (1996).

[14] M. KHONSARI, D. Y. HUA, Thermal EHD Analysis Using a Generalized Non-Newtonian Formulation with Application in Bair-Winer Constitutive-Equation, J. of Tribology, 116, (1994).